Anti-Friction Bearing Systems for Jet Engines

Abstract

This paper presents an overview of anti-friction bearing technology for jet engines with an insight into the physics involved in bearing operations. Major issues affecting the lubricant performance have been discussed. Also presented is a quantitative assessment of parameters, viscosity, temperature and pressure, affecting system performance. Several methods to predict the performance of tribological systems have been highlighted. The information and analyses provided will give the engine design team an efficient evaluation of the bearing systems rectified for certain design parameters.

Nomenclature

	a	Semi-major axis of the Hertzian Contact
	b	Semi-minor axis of the Hertzian Contact
	B	Boundary Lubrication
L		
	E	Elastic Modulus (GPa)
	E	Elastohydrodynamic Lubrication
HL		
	E	Reduced Modulus of Elalsticity
$'$		
	P	Maximum Hertzian Contact Pressure (GPa)
0		
	P	Mean Hertzian Contact Pressure (GPa)
m		
	P	Hertzian Contact Pressure
(r)		
	r	Radius of ball (m)
b		
	r	Radius of disk (m)
d		
	R	Equivalent radius of curvature for Hertzian contact
	R	Average Surface roughness
a		
	R	Maximum peak to valley distance for a given length
max		
	S	Skewness
ku		
	W	Normal Load

1. Introduction

A bearing system is an essential part of a turbo-machinery assembly, it guides/positions components and transmits loads while allowing smooth relative motion. Mechanical losses arising in a gas turbine jet engine incur 10 to 15% of fuel energy [1], these losses are, typically, dominated by the friction generated in bearings. Also, the main aerodynamic losses arising from the fan/turbine blade tip clearances directly depend on the allowances set by the bearing system. Therefore, a careful design/selection of a bearing system is very much of a fruitful task.

Friction is an embedded issue in existing problems across multiple engineering fields including dynamics and control, contact mechanics, aeromechanics, structural dynamics and fracture mechanics. However, the presented research is focused on the engineering discipline "tribology". Tribology deals with the science and technology of lubrication that may achieve friction control and wear prevention of interacting surfaces. Tribological design abides two main principles; 1) prevent contact between rubbing surfaces and 2) regard the separating medium "the lubricant" as an integrated element of machine. A classic example is a ball-bearing or a cam-follower contact. This paper intends to present a critical assessment of tribological factors encompassing bearings.

2. Tribology

2.1 Friction

The friction phenomenon was first explored by Leonardo Da Vinci (1452-1519). He stated that the friction force is doubled as the mass is doubled and the force is independent of the area in contact [2]. The existence of friction was introduced into the world of science by the motion laws of Sir Isaac Newton (1643 -1727) particularly the one that stated 'every object in a state of uniform motion tends to remain in that state of motion unless an external force is applied to it'. The external forces were recognised to be resistive forces i.e. air drag, gravity and the force generated at a surface of contact. The law directly points towards the external forces, i.e. the frictional force that a body experiences in motion.

The frictional phenomenon was first studied experimentally by Guillaume Amontons (1663 - 1705) who discovered that frictional force is dependent on the surface characteristics of the contacting bodies. Later it was Charles Augustine de Coulomb (1736 - 1806) who modelled and formulated the frictional phenomenon based on numerous experimental tests.

2.1.1 Effect of Surface Profile – Roughness

The evolution in tribological sciences has shown that surface profile, particularly the micro/nano geometry, is the most important factor in determining the friction and wear of rubbing surfaces [2]. Therefore, it is vital to examine the surface topography of surfaces under consideration. Herein, four different surface profiles are examined where one is machine polished, two are manually polished using sand papers of different grit sizes to reduce surface roughness of the unpolished standard sample. Figure 1 shows 3-dimensional plots of surface heights for the samples. Unpolished disk samples have the highest surface roughness and the machine polished offers the lowest average roughness. Manually polished samples, P1200 and P600, have moderate roughness values, however, the skewness values are lower compared to the unpolished/machine polished samples, making them a better bearing surface as more lubricant is deposited in the valleys. Furthermore, the density of larger asperities around the surface is higher for the unpolished and machine polished disks compared to the manually polished disks.

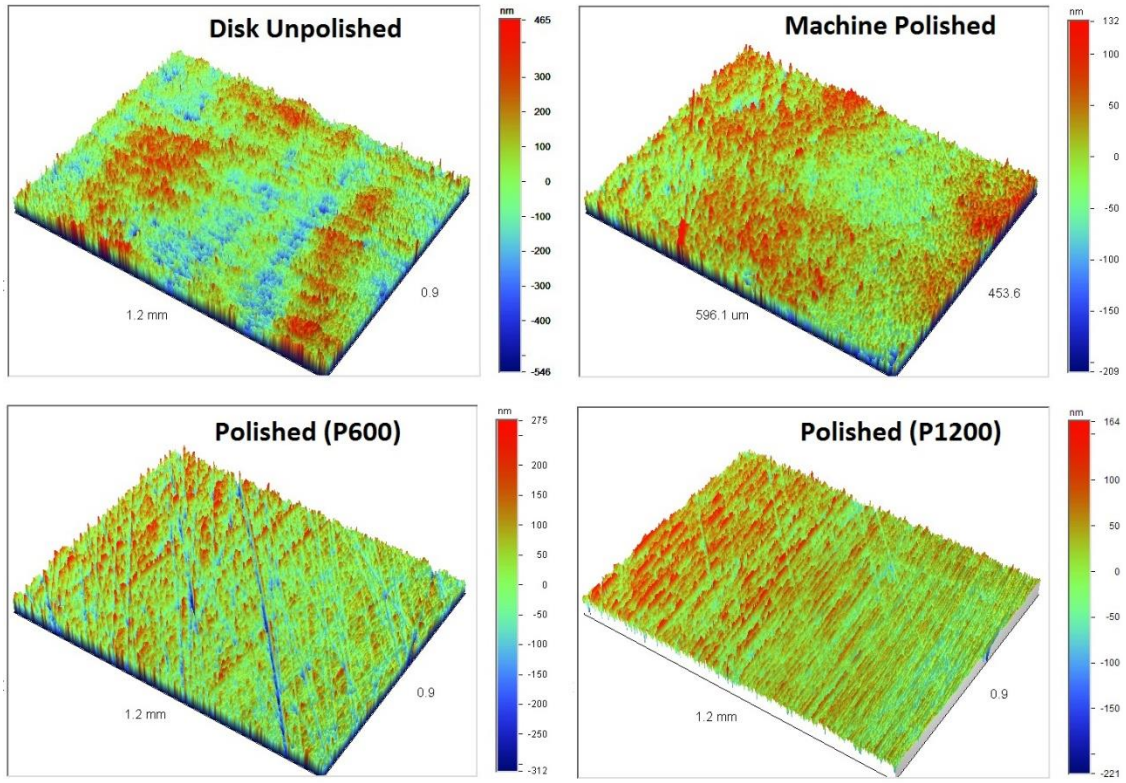

Figure 1: Surface topography of different samples before testing – taken by Wyko NT3300S.

2.2 Lubrication

Lubrication has been the necessity of humans since it started moving goods around, for example moving heavy stones to build the great pyramids or a wheel-cart for conveyance where some form of lubricant was used to reduce the effort. With relatively low speeds vegetable oils/fats proved quite fruitful in reducing friction or the effort for movement.

2.2.1 Lubrication Regimes

The Stribeck diagram, displayed in Figure 2, best defines the friction behaviour of lubrication regimes with regards to the Stribeck number composed of three parameters lubricant viscosity, relative speed of surfaces and the applied normal load/pressure. For high values of Sribeck number, in the hydrodynamic lubrication regime, the friction coefficient increases linearly as the friction is directly caused by the fluid viscous drag and in this regime the viscosity stays constant. In the mixed lubrication regime (or elastohydrodynamic lubrication EHL), as the load increases or the viscosity/speed decreases the fluid film becomes thinner, which subsequently decreases viscous drag or friction coefficient until a minimum is reached. A further drop in Stribeck number leads to metal-to-metal contact and friction coefficient starts to rise. In boundary lubrication a much stronger metal-to-metal contact is formed, the film thickness becomes smaller than the averaged roughness of the surface or the height of the asperities (refer to [3] for further illustration).

It is the phenomenon of metal-to-metal contact that encouraged some early researchers [4, 5] in the field to establish the lubrication regimes with regard to specific film thickness. The specific film thickness is determined by equivalent surface roughness of both surfaces and fluid film thickness. The fluid film thickness measurement, based on EHL film, has been discussed in [6]. The Hamrock and Dowson formula to evaluate film thickness, given in equation (1.1), is based on Hert'z model of contact stresses. This formula defines the minimum specific film thickness h_o / R_x with

regards to surface velocity *U*, normal load *W* and material properties *G*.

$$\frac{h_o}{R_x} = 3.63U^{0.68}G^{0.49}W^{-0.073}(1-e^{-0.68k}) \quad (1)$$

Figure 2 also plots the friction response of a lubricated system against the specific film thickness λ . At higher values of λ the surfaces are separated by fluid film lubrication, the wear is minimal and only occurs due to fatigue from pressure fluctuation in the fluid. Fluid film failure may occur at lower values of $\lambda = 3$ or $\lambda = 5$ [6] and solids may come into partial contact. Mixed lubrication occurs between 1 to 3/4 values of λ , therefore it is sometimes referred to as partial-elastohydrodynamic lubrication. In this regime wear becomes more prominent due to interaction of asperities; also, localised pressure peaks and thermal properties of fluid can cause film breakdown for higher asperities. At the lowest film thickness $\lambda \leq 1$ the fluid film completely breaks down and to minimise friction and wear special boundary lubricants are used [4].

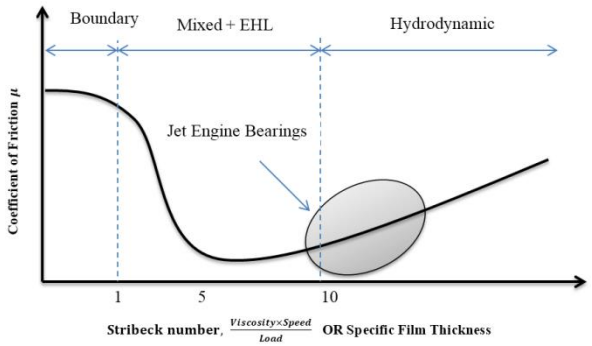

Figure 2: Generic Stribeck Diagram specifying friction response for different lubrication regimes – coefficient of friction vs Stribeck number.

2.2.2 Viscosity-Temperature-Pressure Relationship

In a typical slider bearing arrangement load and temperature are non-constant as the lubricant viscosity depends on temperature, pressure and shear rate. This phenomenon can have significant impact on tribological performance of a system. Figure 3 shows the effect of temperature and pressure on the viscosity of a lubricant, the viscosity rises linearly with pressure and temperature. As mentioned above friction in fluid film lubrication mainly arises from viscos drag, hence, an increase in viscosity implies an increase in friction. This makes the selection of viscosity in a bearing challenging as the dynamic viscosity decreases with temperature and increases with pressure. The viscosity-temperature-pressure relationship is defined by the following equation [8].

$$\ln\frac{\eta}{\eta_0} = (\ln\eta_0 + 9.67) \times \left\{\left(\frac{T-138}{T_0-138}\right)^{-S_0}\left(1+\frac{P}{0.196}\right)^{Z} - 1\right\} \quad (2)$$

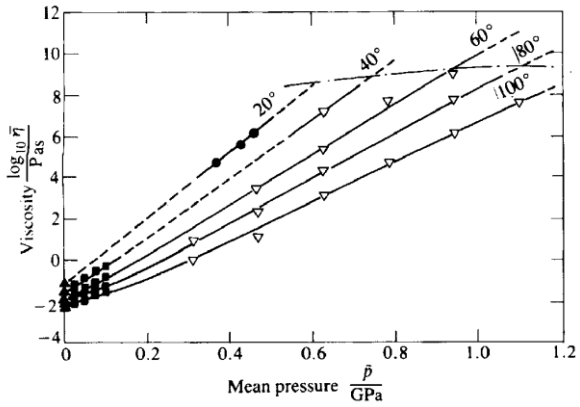

Figure 3: Effect of temperature and pressure on viscosity of a typical lubricant [9].

2.2.3 Lubricant Contamination

Lubricants can contain solid particles generated by abrasion/adhesion friction mechanisms or entrain from surrounding environment. . The solid particles cause a dent on the surface creating a pressure filed that due to nonlinear film pressure causes fatigue problems. These particles cause surface damage and wear that in some cases can lead to total system failure. Experimental study [10] has shown that sand particles in oil suspensions, with high rate of sliding, can cause significant wear damage within a few operating cycles and eventually lead to system failure. Theoretical and experimental studies [11] have shown that lubricant contamination is prominent in EHL regime with moderate film thickness and the dents on surface alter the actual film thickness.

Condition monitoring and quantification of oil contamination is crucial to tribological

performance of a machine and ferrography (microscopic examination) has been the tool to analyse wear in oils. However, recently, optical ferroanalyzer in addition to ferrograph has been shown to estimate total contamination of oil, increasing reliability of tribosystem condition monitoring [12].

2.2.4 Jet Engine Lubrication

Generally, there are three/four compartments for bearings positioned just behind the main fan, at the middle before the combustor and at the rear behind the turbine. The bearings in jet engines are actively lubricated to operate in EHL/hydrodynamic lubrication regime, a typical jet engine lubrications is shown in Figure 4. The lubricant oil also acts as a coolant and transposes the wear particles.

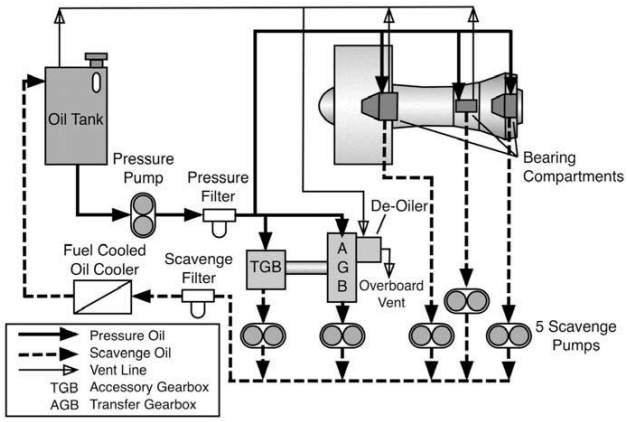

Figure 4: A schematic of typical Jet-Engine Lubrication System [13]

2.3 Concentrated Contacts and Wear

Machine elements with low conformity, such as ball bearings, cams and gears, come into surface-to-surface contact where the contact pressure distribution changes due to the deformation of the nominal geometry. In order to quantify the pressure distribution and contact deformation standard Hertzian elastic contact equations are applied and the simplified contact geometry is shown in Figure 5.

Assuming circular contact area at the ball-disk interface relationships for the Hertzian contact pressure, deformation and the radius of the contact (the semi-major axis of the contact) are plotted in Figure 6. From the figure it can be seen that as the normal load is increased the contact pressure and deformation increase with a certain relationship and the contact area expands.

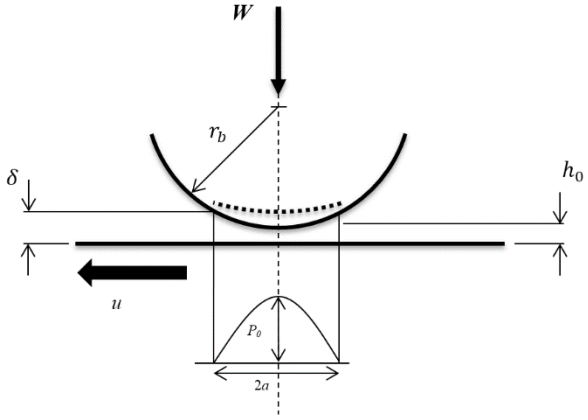

Figure 5: Hertzian Elastic Contact Mechanics Illustration.

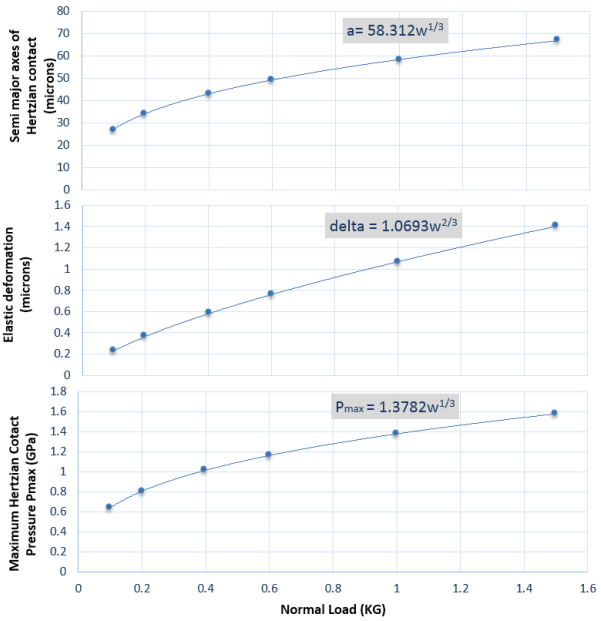

Figure 6: Relationships of Hertzian contact pressure, deformation and the contact profile.

Two bodies in contact may change their geometry due to wear and the change depends on the material properties particularly the Hardness. Surface wear can attenuate geometrical profile at micro level which can directly influence performance parameters including film thickness and Hertzian contact pressure distribution. For point contact, for example ball-on-disk, the change in contact configuration is directly dependent on the hardness of the materials in contact [14, 15].

1. $H_{ball} > H_{disk}$ - only disk wears
2. $H_{ball} < H_{disk}$ - only ball wears
3. $H_{ball} \approx H_{disk}$ - both ball and disk wear (the amount depends on the roughness)

Figure 7 shows change in contact pressure with sliding distance, or wear, for coupled materials (same material for ball and disk) with different hardness values. The contact pressure drops with sliding distance agreeing to an inverse-power relationship. After ~50 meters of sliding distance the pressure drop is minimal and converges to a constant value. Furthermore, for materials with lower values of Hardness and elastic modulus E the pressure drop is higher comparably.

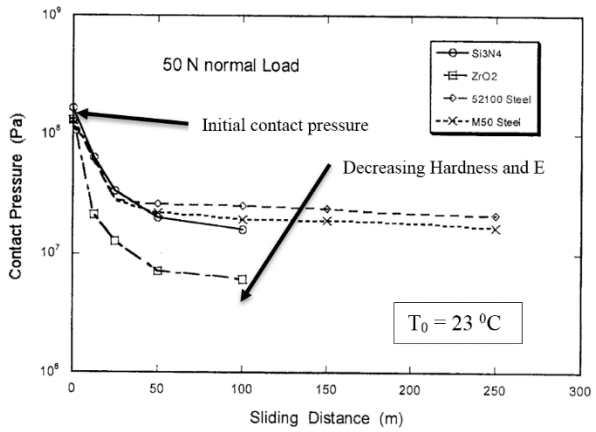

Figure 7: Change in contact pressure with sliding distance for different materials using standard pin-on-disk apparatus {derived from [16]}.

3. Selecting a Bearing System

A bearing system in a jet engine has to locate the shaft and support the axial/radial loads with minimum frictional losses. Figure 8 shows a typical loading of the main shaft in a jet engine, the incremental loading on the shaft from intake to exhaust changes its direction, however, the net axial force is the thrust in flight direction. This implies that a thrust bearing has to support the thrust load, allow large rotational speeds, typically 6,000 to 30,000 rpm, and keep the shaft in place.

Once the loading and rotational speeds are known an appropriate bearing system can be selected from Figure 9. Most commonly jet engines utilise lubricated roller bearings as shown in Figure 10.

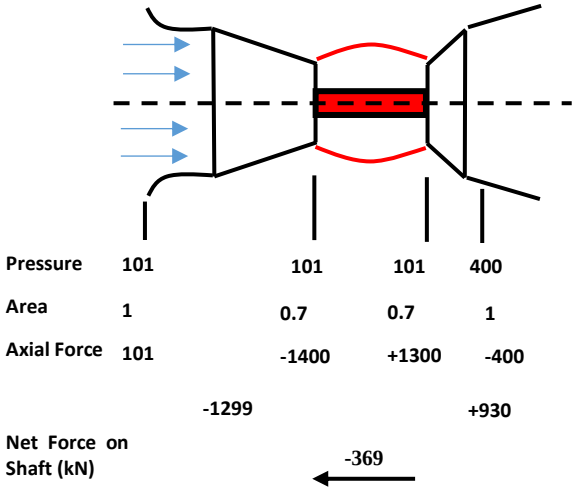

Figure 8: Typical shaft loading of a jet engine – all the forces and pressures in kN and kPa respectively.

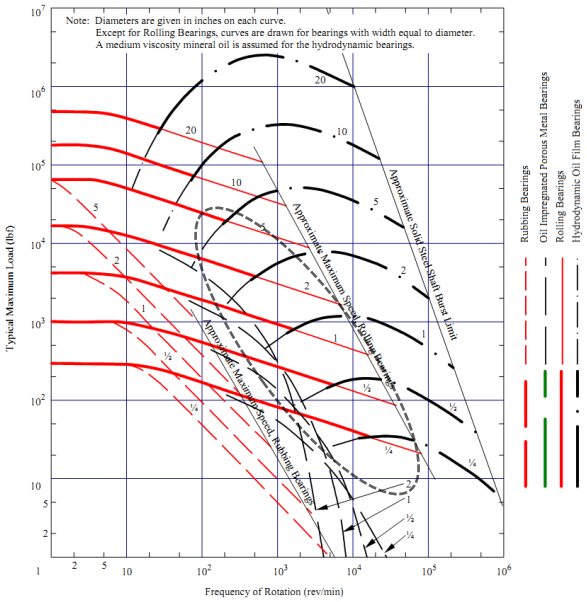

Figure 9: General guide to bearing selection [14].

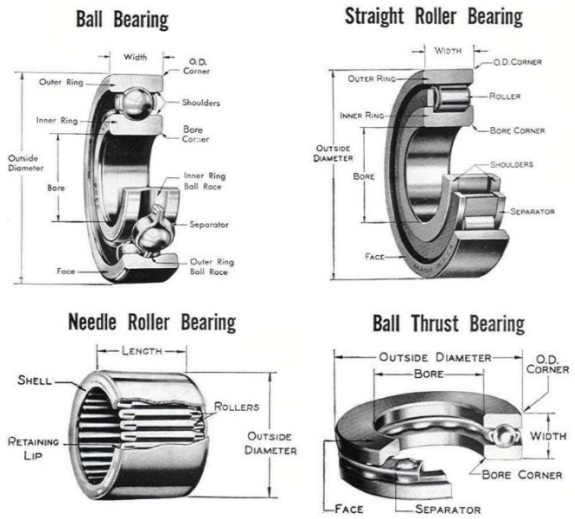

Figure 10: Different kinds of roller bearing [17].

4. Potential Design Parameters to Improve Tribological Performance

4.1 Material Selection

From a tribological perspective material is the most important design parameter as the mechanical properties of the material define the pressure distribution which defines the friction characteristics. Figure 11 displays friction behaviour of bronze-based materials with different mechanical properties. Initially, at start-up, no certain relationship can be defined, however, as the steady-state is reached best friction performance is portrayed by specimen M-2 with relatively low young's modulus and elastic deformation.

Ideally, a bearing material must have compressive strength to withstand the film pressure loading and fatigue strength to bear the cyclic loading and the changing temperatures. However, at the same time it should possess an elastic modulus to allow elastic deformation and allow the wear particles to flow. In [18] a systematic methodology has been developed to select an appropriate material for the bearing. The method ranks the materials with respect to friction coefficient, contact parameters and the wear rate under the conditions of boundary lubrication. Copper-lead and bronze-lead materials are said to meet most of the tribological criterion for a bearing.

Some new materials are emerging to improve friction and wear performance of bearings. In [19] lead-free (bismuth) and tin based materials are examined, their friction and wear behaviour is displayed in Figure 12. The bismuth based material (material B) offers slightly better friction properties and much better wear properties compared to the conventional material (material A).

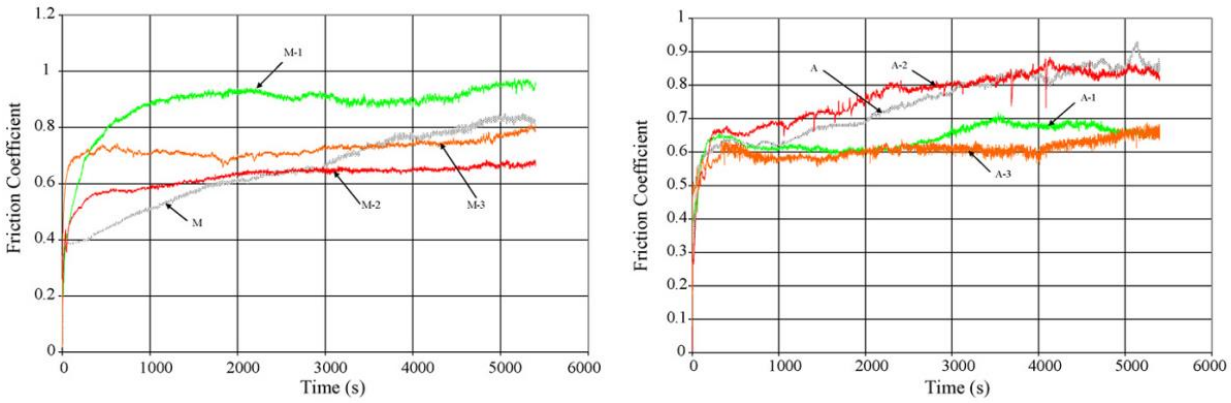

Specimen ID	Hardness (GPa)	Young's modulus (GPa)	Max. deformation in loading (nm)	Max. deformation in unloading (nm)	Plastic deformation (%)	Elastic deformation (%)
M	1.53	95.85	1291.67	1183.89	91.66	8.34
M-1 matrix	1.42	107.35	1360.43	1253.31	92.13	7.87
M-1 particle	12.19	233.00	503.65	348.77	69.25	30.75
M-2 matrix	1.43	94.29	1371.49	1258.59	91.77	8.23
M-2 particle	10.72	227.42	531.07	384.54	72.41	27.59
A	1.50	106.67	1298.04	1196.25	92.16	7.84
A-1 matrix	2.39	111.38	1052.01	932.26	88.62	11.38
A-1 particle	12.18	222.64	504.11	347.74	68.98	31.02

Figure 11: Friction coefficient vs. time and mechanical properties for premixed bronze-based specimens and prealloyed bronze-based specimens [20].

	Composition			
Material	Overlay	Interlayer	Lining	Steel
A	Pb, 8%; Sn, 2%; Cu, 14 μm	Ni, 2 μm	Cu, 23%; Pb, 3%; Sn, ~0.5 mm	Mild steel
B	Bi, 5 μm	Ag, 5 μm	Cu, 10%; Sn, 4%; Bi, ~0.5 mm	Mild steel
C	Sn, 3%; Cu, 18 μm	Ni, 2 μm	Cu, 23%; Pb, 3%; Sn, ~0.5 mm	Mild steel

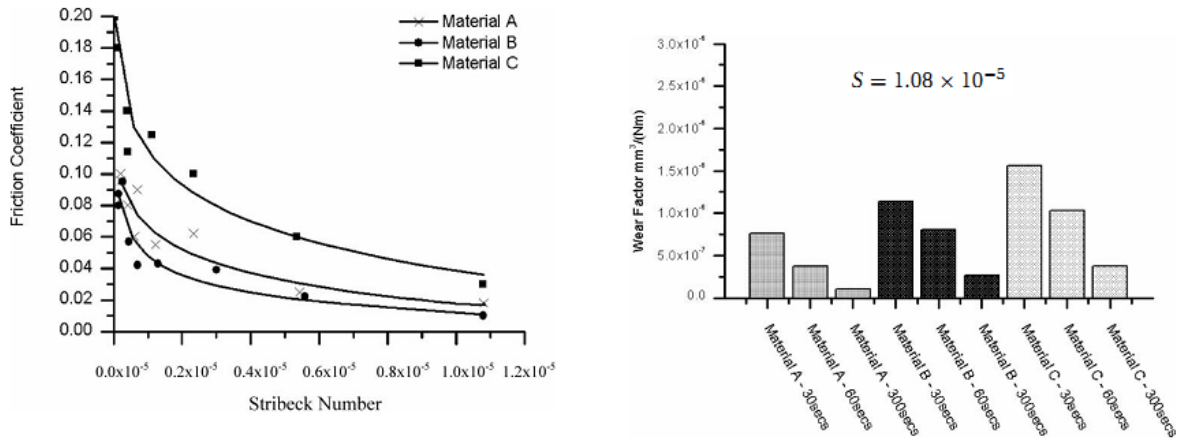

Figure 12: Effect of materials on friction and wear performance [14].

4.2 The effect of grain size on transition from BL to EHL regime

Fundamental mechanical properties of steel, including hardness, yield strength, the ductile-brittle transition temperature and susceptibility to environmental embrittlement can be improved by refining the grain size. The well-known Hall-Petch effect quantifies the improvements on properties with respect to $d^{-1/2}$ where d is the grain size [21]. Figure 13 displays the effect of grain size on mechanical properties of different materials, increasing the grain size enhances the ductile-brittle temperature transition (DBTT), but reduces the yield strength.

Another interesting phenomenon of grain size is the stress-strain relationship under dynamic loading. Figure 14 shows that the magnitude of stress varies nonlinearly with strain for different material samples. Particularly, for compression loading the fluctuation in stress more rapid compared to the tensile loading. An important point to be noted here is that for interacting surfaces the loading is predominantly compressive/dynamic and that changes with the grain size which implies that the friction response will vary with the grain size.

Grain size does not only influence the mechanical properties, it also has significant effect on friction response of a lubricated system as shown in Figure 15, increasing the grain size shifts the transition from mixed to BL to the right. However, the maximum and the minimum friction coefficients remain unchanged. The occurrence of BL regime, shift to right, with increasing grain size is probably due to the fact that for larger grain sizes the mean film thickness increases; however, the asperities come into contact leaving the system in BL regime even at higher values of λ .

The grain size effect on friction/wear has been studied, theoretically and experimentally, for many materials including aluminium/magnesium alloys and ceramics [22, 23, and 24]. However, for an unknown reason the material steel hasn't been examined with regard to its grain size and friction/wear response

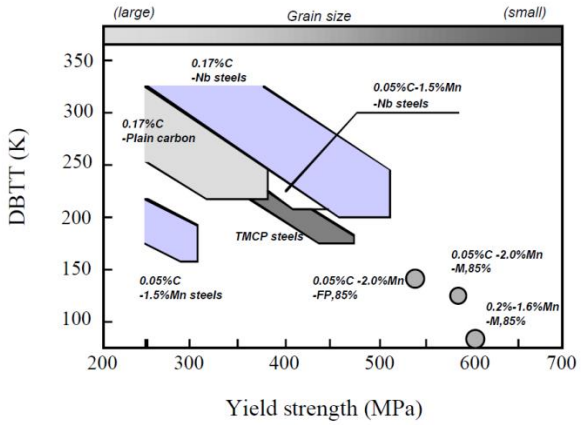

Figure 13: Effect of grain size on mechanical properties of different materials [25].

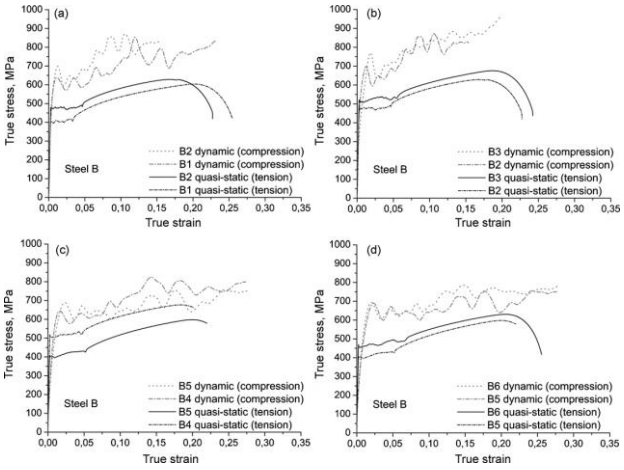

Figure 14: Flow stress comparison for steel [26].

.

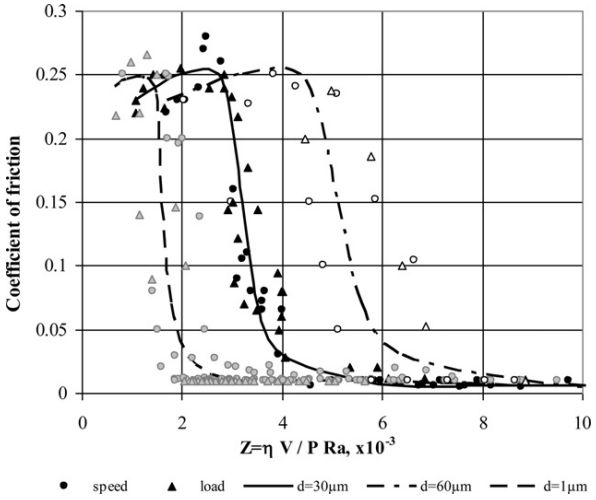

Figure 15: Effect of grain size on Stribeck diagram for copper [27].

5. Conclusions

An overview of bearing systems has been presented with the following findings:

- Bearing systems can be rectified based on the load and rotational speed criteria – for jet engines it's mostly lubricated roller bearings.
- Surface topography or micro-geometry of the surfaces in contact is of great importance – the surface parameters including average surface roughness R_a, skewness and R_{max} directly influence friction behaviour and the wear characteristics of the system. This implies that machining process for a bearing is crucial
- Average surface roughness has a significant impact on the onset and trend of mixed lubrication regime
- Average surface roughness does not provide a full account of film thickness and friction behaviour in ML, the surface parameter R_{max} must also be considered.
- Mixed to boundary lubrication transition is contact pressure (or normal load) dominated
- The generic characteristic number the Lambda ratio is inappropriate for the analysis of lubricated concentrated contacts in the mixed lubrication regime.

6. References

[1] Stachowiak, W., and Bachelor, A. W., (2000): Engineering Tribology (2nd ed.).Boston, MA: Butterworth-Heinemann, an imprint of Elsevier Science.

[2] Olsson, H., et al., *{Friction models and friction compensation}.* Eur. J. Control, 1998. **4**(3): p. 176-195.

[3] Cameron, A., *Basic Lubrication Theory*. 1971, London: Longman Group Limited.

[4] Hutchings, I.M., *Tribology: friction and wear of engineering materials.* Edward Arnold, Great Britain, 1992.

[5] Neale, M.J., *The Tribology Handbook 2nd Ed*. 1997, USA: Butterworth-Heineman.

[6] Dowson, D., *Elastohydrodynamic and microelastohydrodynamic lubrication.* Wear, 1995. **190**: p. 125-138.

[7] Bayer, R.G., *Mechanical Wear Prediction and Prevention.* Marcel Dekker, USA, 1994.

[8] Gold, P.W., et al., *Viscosity–pressure–temperature behaviour of mineral and synthetic oils.* Journal of Synthetic Lubrication, 2001. **18**(1): p. 51-79.

[9] Evans, C.R. and K.L. Johnson, *The Rheological Properties of Elastohydrodynamic Lubricants.* Proceedings of the Institution of Mechanical Engineers, Part C: Journal of Mechanical Engineering Science, 1986. **200**(5): p. 303-312.

[10] Sari, M.R., A. Haiahem, and L. Flamand, *Effect of lubricant contamination on gear wear.* Tribology Letters, 2007. **27**: p. 119-126.

[11] Ko, C.N. and E. Ioannides, *Debris denting – The associated residual stresses and their effect on the fatigue life of sliding bearing, an FEM analysis.* Proceedings of 15th Leeds-Lyon Symposium on Tribology. -Amsterdam, 1989: p. 199-207.

[12] Myshkin, N.K., et al., *Wear monitoring based on the analysis of lubricant contamination by optical ferroanalyzer.* Wear, 2003. **255**(7–12): p. 1270-1275.

[13] Jet Engine Oil System Part one. ExxonMobil Aviation Lubricants. www.exxonmobil.com {accessed 18-03-2014}

[14] ASTM G 99 - 95a: Standard test method for wear testing with a pin-on-disc apparatus.

[15] Wong, P.L., Huang, P., Wang, W. and Zhang, Z., "Effect of geometry change of rough point contact due to lubricated sliding wear on lubrication", Tribology Letters, Vol. 5, 1998, pp. 265-274.

[16] Ajayi, O.O. and Erck, R.A. "Variation of nominal contact pressure with time during sliding wear. Technical Report, DE2002-799783, Energy Technology Division Argonne National Laboratory, 2001.

[17] Khonsari, M.M., and Booser E. R., An Engineering Guide For Bearing Selection, Tribology and Lubrication Technology, 2004

[18] Evans, C.R. and K.L. Johnson, *The Rheological Properties of Elastohydrodynamic Lubricants.* Proceedings of the Institution of Mechanical Engineers, Part C: Journal of Mechanical Engineering Science, 1986. **200**(5): p. 303-312.

[19] Kerr, I., et al., *Friction and wear performance of newly developed automotive bearing materials under boundary and mixed lubrication regimes.* Proceedings of the Institution of Mechanical Engineers, Part J (Journal of Engineering Tribology), 2007. **224**(J3): p. 321-31.

[20] Tavakoli, A., R. Liu, and X.J. Wu, *Improved mechanical and tribological properties of tin-bronze journal bearing materials with newly developed tribaloy alloy additive.* Materials Science & Engineering: A (Structural Materials: Properties, Microstructure and Processing), 2008. **489**(1-2): p. 389-402.

[21] Cottrell, A.H., *The Mechanical Properties of Matter*. 1964, New York: Wiley.

[22] El-Raghy, T., P. Blau, and M.W. Barsoum, *Effect of grain size on friction and wear behavior of Ti3SiC2.* Wear, 2000. **238**(2): p. 125-130.

[23] Farhat, Z.N., et al., *Effect of grain size on friction and wear of nanocrystalline aluminum.* Materials Science and Engineering: A, 1996. **206**(2): p. 302-313.

[24] Feng, X., H. Liu, and S. Suresh Babu, *Effect of grain size refinement and precipitation reactions on strengthening in friction stir processed Al–Cu alloys.* Scripta Materialia, 2011. **65**(12): p. 1057-1060.

[25] Morris, J.W., Jr, *The Influence of Grain Size on the Mechanical Properties of Steel.* DOE Scientific and Technical Information, 2002.

[26] Muszka, K., P.D. Hodgson, and J. Majta, *Study of the effect of grain size on the dynamic mechanical properties of microalloyed steels.* Materials Science and Engineering: A, 2009. **500**(1–2): p. 25-33.

[27] Moshkovich, A., et al., *The effect of Cu grain size on transition from EHL to BL regime (Stribeck curve).* Wear, 2011. **271**(9–10): p. 1726-1732.